The coupled seismoelectric wave propagation in porous media: Theoretical background

Mehran Gharibi, R. Arief Budiman, Robert R. Stewart, and Laurence R. Bentley

ABSTRACT

Seismic and electromagnetic disturbances are coupled in saturated porous materials through electrokinetic coupling. Two types of seismoelectric signals are generated when a seismic wave propagates through a homogeneous multi-layer porous medium. The first type of the seismoelectric response is generated by a stationary charge separation, in a reference frame moving with the wavefront. This stationary charge separation is analogous to a constant electric dipole and does not radiate electromagnetic waves. The second type of the seismoelectric response is generated when the spherically spreading wavefront impinges on an interface having contrast in mechanical or electrical properties in which a time-varying charge separation is induced. This time-dependent charge separation radiates electromagnetic (EM) energy, which would be detected almost simultaneously across the surface receivers.

To enhance the weak signal of the observed seismoelectric signals, processing procedure includes suppressing of the powerline large amplitude harmonic interferences as well as the seismoelectric response type separation. Powerline harmonic interference can be estimated and removed from the data using block or sinusoid subtraction techniques. Discriminating between the first and second type of the seismoelectric EM responses can be done using F-K filtering, because of the distinct near simultaneous arrival characteristic of the interface EM response. Another possible separation technique is a self-deconvolved prediction error filter. This technique is similar to the algorithms that are used for multiple attenuation in reflection seismic data.

INTRODUCTION

When compressional (P) or shear (S) seismic waves generated by an impulsive source such as hammer blow or explosion propagate through a fluid saturated porous medium, a small amount of relative motion between the solid matrix and pore-fluid is introduced. This relative motion in the presence of an electric double layer near the solid-fluid contact surface (Figure 1) causes a charge separation that in turn creates an electric field, which accompanies the seismic wave. For compressional waves, accumulation of charge also contributes to the charge separation which give rise to an internal electric field in the propagation direction (Haartsen and Pride, 1997). In homogenous porous materials, the current that is created by counter ion charge accumulation balances the current set up by relative charge separation (streaming current) caused by fluid movement. Therefore outside of the wave the total current is zero and independent electromagnetic waves are not generated (Pride and Haartsen, 1996). However, there is an internal constant electric field confined within and traveling with the compressional wave that can be recorded with a dipole antenna when seismic wave is passing through (Figure 2). The velocity and frequency of the recorded electric field will be that of the seismic wave velocity $v=\lambda f$, where f is dominant frequency and λ is wavelength.

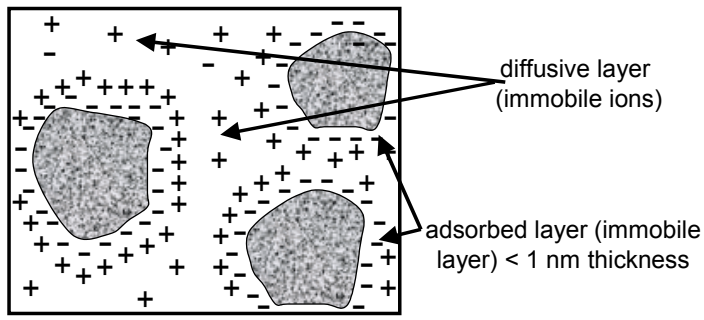

FIG. 1. Electrical double layer in fluid-saturated porous medium at the grain scale.

For shear waves, accumulation of charge does not exist but the relative fluid-matrix movement induces streaming current that generate small magnetic and electric fields due to induction. These two fields are confined within and travel with the seismic wave. A magnetometer, that is not sensitive to motion, can be used to measure magnetic field component inside the shear wave.

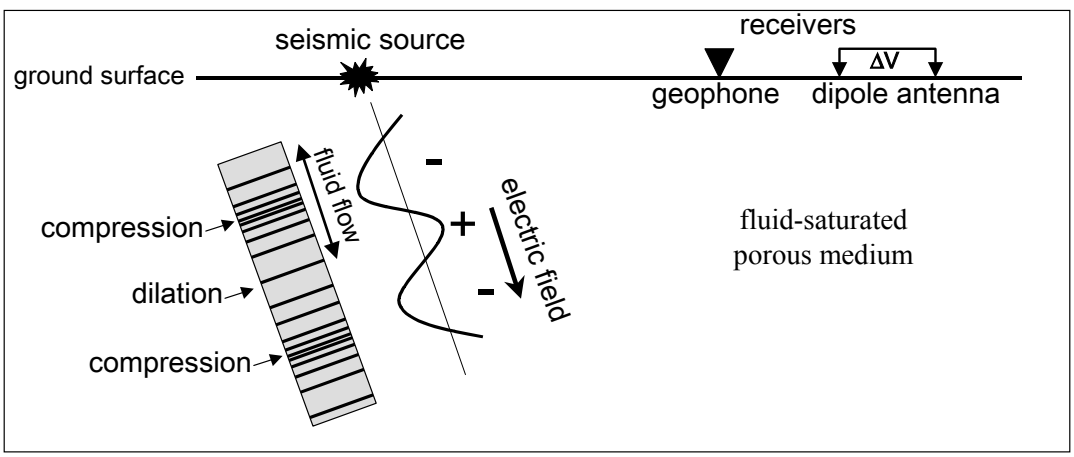

FIG. 2. Compressional seismic wave and its associated seismoelectric response in a homogeneous fluid-saturated porous medium.

Waveforms and amplitudes of the electric and magnetic fields generated by traveling P and S wave, respectively, are controlled by the electrical and mechanical properties of the saturating fluid. Transfer functions between seismic waves and the corresponding electric or magnetic fields can be used to estimate some of these properties (Garambois and Dietrich, 2001). The electric fields accompanying the P waves are mainly sensitive to electric properties of pore fluid such as salinity and dielectric permittivity. The transfer function between S waves and the corresponding magnetic fields show a distinct dependence on the viscosity of the saturating fluid (Mikhailov et. al., 2000).

In layered media, propagation of the seismic wave gives rise to a second-order effect. When the downgoing seismic wave traverses an interface between two porous media having contrast in mechanical and/or electrical properties a time-varying charge

separation is induced (Figure 3). This charge separation is present only while the hemispherical wavefront crosses a boundary separating two media with different streaming potential coefficients or different fluid properties (e.g. oil-water contacts). The charge disturbance oscillates at the elastic wave frequency within the circular zones (Fresnel zones) centred on the position of the surface seismic source. The radius of the circular Fresnel zones is a function of the seismic wave wavelength and is approximated as $r=(z\lambda/2)^{1/2}$ (Beamish and Peart, 1998). The coherent regions of displacement within the first Fresnel zone act as a time-dependent vertical electric dipole (VED) radiating electromagnetic (EM) energy, independently of the exciting seismic wave, which would be detected almost simultaneously at the surface using an array of electric antennas. The phase reversal of the observed VED field oscillations across the plane of symmetry (surface seismic source position) makes it possible to distinguish the VED field in the presence of other electromagnetic noise.

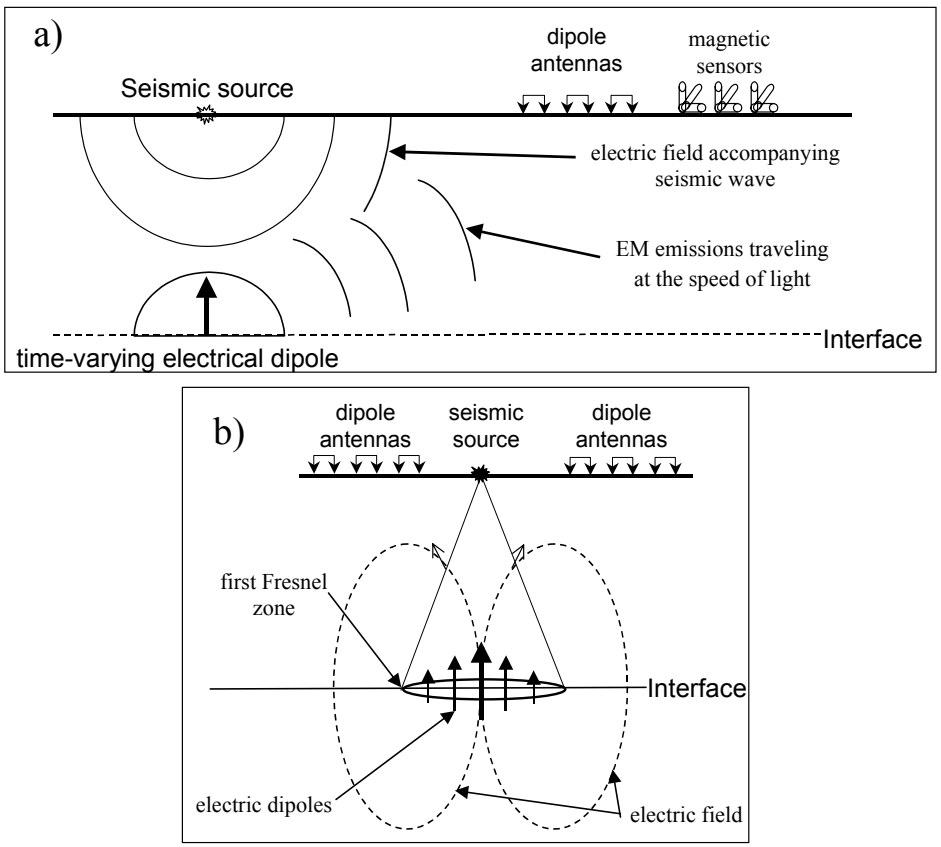

FIG. 3. a) Time-varying electric dipole generated at the interface and its EM radiation, b) Phase reversal of the observed EM field across the plane of symmetry.

The potential field distribution observed at the surface can adequately be approximated as that of a dipole. The magnitude of the dipolar field is expressed by its dipole moment, the product of current and volume of the charge separation which is determined by the area of the first Fresnel zone and the thickness of Biot slow wave attenuation length. The Biot slow wave is a converted elastic wave that is generated when seismic waves encounter contrast in acoustic impedance and is principally responsible for

the large charge separation at layer interface and the resulting EM emission (Biot, 1962, 1956; Pride, 1994; Pride and Haartsen, 1996). The Biot slow wave is a diffusive pressure wave at the seismic frequency band and it has an attenuation length of much less than 1 m (Thompson and Gist, 1993).

The range of the electrical conductivity of the earth materials combined with the acoustic frequency band used in seismic experiments dictates that the EM fields generated at an interface is diffusive, i.e. the displacement current is negligible compare to the conduction current. The wavelength of the diffusive EM radiation is $\lambda=(4\pi/\sigma\mu f)^{1/2}$, where σ is the conductivity, μ is the magnetic permeability, and f is the frequency. The diffusive EM wavelength is usually several times larger than the depth to the interface. In this case, large electromagnetic skin depth, defined by $\delta=500(\sigma f)^{-1/2}$, where σ is the conductivity, and f is the frequency, assures a minor amplitude attenuation of the EM energy as it returns to the surface. The seismic energy reflected from the same interface loses its higher frequency content on its return to the surface. This implies that the converted EM radiation will have higher vertical resolution compared to its corresponding seismic wave.

DATA PROCESSING

In multi-layer media, several interface EM radiations from the subsurface interfaces are generated. Since the EM signals from each interface propagate to the surface at the speed of light they occur in the record simultaneously across the surface array at the one-way transit time of the downgoing seismic wave. These signals can be masked by the signals that are associated with the first type of seismoelectric response that travel within the seismic waves. Furthermore, the small field or laboratory seismoelectric signals are usually contaminated by larger ambient electromagnetic noise. The sequence of data processing procedures should primarily include band-pass filtering as well as suppressing the powerline harmonic interference which usually dominants the data because of the large amplitude. Butler and Russell (1993) described two processing techniques, block subtraction and sinusoid subtraction, to estimate and subtract multiple powerline harmonic noise without attenuation of the signal of interest. In block subtraction, the powerline harmonic noise is estimated from an interval of the record over which the non-harmonic components are assumed to be negligible. The powerline harmonic will then be removed by shifting and subtracting the noise block from the record. The second method uses a least-squares algorithm to estimate harmonic noise amplitude and phase from the data. The harmonic noise will then be suppressed by subtracting sinusoids having the estimated frequency, amplitude, and phase from the record.

To enhance and discriminate between the second type of the seismoelectric EM response, generated in the multi-layer interfaces, and the first type of the response that accompany the seismic waves further processing is required. The distinct polarity reversal characteristic of the second type seismoelectric response allows a straightforward identification in seismoelectric records. However, to separate the responses from the deeper interfaces that are usually hidden inside the first type seismoelectric energy a more advance data processing is required. Lack of normal moveout in this type of the seismoelectric response suggests that F-K filtering can be an option to separate them from the first type of the response. However, in practice, the small amplitude of the

interface EM response at large offsets compared to the first type of response, could restrict performance of this type of transformation.

Another technique that can be used to separate the signal of interest in seismoelectric data is based on prediction-error filters. These filters are widely used in geophysical processing to attenuate multiples in reflection seismic record (e.g. van Dedem and Verschuur, 2001). If one assumes that the seismoelectric data is the sum of a desired energy (signal) and of an undesired energy (noise), then a prediction error filter for signal or noise can be estimated from the data so that when it operates on the data signal or noise component, respectively, the prediction error will be zero. Soubaras (1994) describes an algorithm that computes the noise component by filtering the data with the self-deconvolved prediction error filter. The filter is a multi-notch filter that operates like a projection operator having eigenvalues of 0 or 1. In this case, the prediction error filter incorporated in the self-deconvolved prediction error filter is estimated from the data by minimizing the projection error instead of prediction error. The algorithm uses an efficient recursive computation in time domain and provides a candidate to effectively separate the predictable component of the seismoelectric data, the horizontal event associated with the interface EM response, from the first type component of the seismoelectric response, which is considered here as noise. This response separation procedure is crucial before any interpretation of the seismoelectric data or other transfer function estimations can be performed.

Close correlation between the seismic reflection data and the first type of the seismoelectric response suggests that seismic data could be used as part of the prediction filter calculation in seismoelectric response separation process. In this case, phase shift between the seismic response and the seismoelectric response should be considered in filter design. Lack of documented literatures and experiences in this regard recommend that further studies need to be undertaken to determine the applicability of the method.

MODEL

We follow the derivation of the seismoelectric model by Pride (1994). It is assumed that the solid phase is insulating, so that it does not have electrical point charge. The total electric charge, including the electric dipole field, thus obeys

$$\nabla \cdot \mathbf{D}_s = 0, \tag{1}$$

where $\mathbf{D}_s = \varepsilon \mathbf{E}_s$ with ε being the dielectric constant. The electric field in the solid phase is accompanied by the magnetic field:

$$\nabla \times \mathbf{E}_s = -\dot{\mathbf{B}}_s. \tag{2}$$

The third Maxwell's equation for the solid phase tells us that the EM wave's magnetic field has zero divergence:

$$\nabla \cdot \mathbf{B}_s = 0, \tag{3}$$

while the fourth one specifies how the magnetic field moves together with the electric field:

$$\nabla \times \mathbf{H}_s = \dot{\mathbf{D}}_s . \tag{4}$$

The magnetic field $\mathbf{H}_s$ in the solid phase is the sum of the electromagnetic wave and the magnetization field: $\mathbf{H}_s = \mathbf{B}_s - 4\pi\mathbf{M} = \mathbf{B}_s - 4\pi\chi\mathbf{H}$; this is often written as $\mathbf{B}_s = \mu\mathbf{H}_s$, where μ is called magnetic permeability.

For the fluid phase, the charged ions will act as the source of the point-charge distribution, so that

$$\nabla \cdot \mathbf{D}_f = \sum_l ez_l N_l , \tag{5}$$

where $e = \pm q$ is the unit charge for either negative or positive ion, z_l is the valency of the ion, and N_l is the number of lth ion. The fluid phase's magnetic field $\mathbf{B}_f$ and the electric field $\mathbf{E}_f$ are defined by

$$\nabla \cdot \mathbf{B}_f = 0, \tag{6}$$

$$\nabla \times \mathbf{E}_f = -\dot{\mathbf{B}}_f . \tag{7}$$

The spatial change in the fluid phase's magnetic field is following by the change in the electric field and the current density:

$$\nabla \times \mathbf{H}_f = \dot{\mathbf{D}}_f + \mathbf{J}_f , \tag{8}$$

where

$$\mathbf{J}_f = \sum_{l=1}^{L} ez_l (-D_l \nabla N_l + ez_l b_l N_l \mathbf{E}_f + N_l \dot{\mathbf{u}}_f)$$

The current density has thus three terms; they are, respectively,

- diffusion current due to ionic density gradient,
- drift velocity from the electric field,
- inertial velocity of the ionic species.

Equations (1)-(8) and four boundary conditions at the solid-fluid interface:

$$\mathbf{n}\cdot(\mathbf{B}_s-\mathbf{B}_f)=0, \tag{9}$$

$$\mathbf{n}\cdot(\mathbf{D}_s-\mathbf{D}_f)=Q, \tag{10}$$

$$\mathbf{n}\times(\mathbf{E}_s-\mathbf{E}_f)=0, \tag{11}$$

$$\mathbf{n}\times(\mathbf{H}_s-\mathbf{H}_f)=Q\dot{\mathbf{u}}_s, \tag{12}$$

$$\mathbf{n}\cdot\mathbf{J}_f=\dot{Q}. \tag{13}$$

define the microscopic equations governing the propagation of EM waves inside the solid and fluid phases and how they interact with ions and produce current density.

Temporal linear stability analysis can be performed to these governing equations by assuming

$$Q(t)=Q^0+q(\omega)e^{-i\omega t}, \tag{14}$$

$$N_l(t)=N_l^0+n_l(\omega)e^{-i\omega t}, \tag{15}$$

$$\mathbf{E}_\xi(t)=\mathbf{E}_\xi^0+\mathbf{e}_\xi(\omega)e^{-i\omega t}, \tag{16}$$

$$\mathbf{H}_\xi(t)=\mathbf{H}_\xi^0+\mathbf{h}_\xi(\omega)e^{-i\omega t}. \tag{17}$$

The steady state fields for the solid phase are zero: $\mathbf{B}_s^0=0$, $\mathbf{E}_s^0=0$, while the first harmonic fields obey

$$\nabla\cdot\mathbf{e}_s=0, \tag{18}$$

$$\nabla\cdot\mathbf{b}_s=0, \tag{19}$$

$$\nabla\times\mathbf{e}_s=i\omega\mathbf{b}_s, \tag{20}$$

$$\nabla\times\mathbf{h}_s=i\omega\mathbf{d}_s. \tag{21}$$

For the fluid phase, $\mathbf{B}_f^0=0$, while $\mathbf{E}_s^0$ obeys

$$\nabla\times\mathbf{E}_f^0=0, \tag{22}$$

$$\varepsilon_0\kappa_f\nabla\cdot\mathbf{E}_f^0=\sum_l ez_lN_l^0, \tag{23}$$

$$-\sum_l ez_lD_l\nabla N_l^0+\sum_l ez_lb_lN_l^0\mathbf{E}_f^0=0, \tag{24}$$

Eq. (22) states that $\mathbf{E}_f^0$ is a conservative field: $\mathbf{E}_f^0=-\nabla\Phi^0$, where Φ^0 is the electrostatic potential in the fluid phase. Hence, Eq. (23) produces the standard Poisson-Boltzmann equation governing the potential distribution of an electrolytic fluid. The solution is

$$N_l^0 = N_l \exp(-\frac{ez_l}{\kappa T}\Phi^0), \tag{25}$$

which satisfies Eq. (24). The first harmonic fields in the fluid phase satisfy

$$\varepsilon_0 \kappa_f \nabla \cdot \mathbf{e}_f = \sum_l ez_l n_l, \tag{26}$$

$$\nabla \cdot \mathbf{b}_f = 0 = \nabla \cdot \mathbf{h}_f, \tag{27}$$

$$\nabla \times \mathbf{e}_f = i\omega\mu_0 \mathbf{h}_s, \tag{28}$$

$$\nabla \times \mathbf{h}_f = -i\omega\varepsilon_0\kappa_f e_f + \mathbf{J}_f, \tag{29}$$

where

$$\mathbf{J}_f = \sum_l ez_l[-D_l \nabla n_l + ez_l b_l N_l^0 \mathbf{e}_f + ez_l b_l \mathbf{E}_f^0 n_l + N_l \dot{\mathbf{u}}_f].$$

The boundary conditions at the interface clearly become*

$$\mathbf{n} \cdot (\mathbf{b}_s - \mathbf{b}_f) = 0, \tag{30}$$

$$\mathbf{n} \cdot (\mathbf{d}_s - \mathbf{d}_f) = 0, \tag{31}$$

$$\mathbf{n} \times (\mathbf{e}_s - \mathbf{e}_f) = 0, \tag{32}$$

$$\mathbf{n} \times (\mathbf{h}_s - \mathbf{h}_f) = Q^0 \dot{\mathbf{u}}, \tag{33}$$

$$\mathbf{n} \cdot \mathbf{J}_f = 0, \tag{34}$$

The mechanical equation is the standard Newton's second law expressed by

$$-i\omega\rho_f \dot{\mathbf{u}}_f = \nabla \dot{\tau}_f + \sum_l ez_l (N_l^0 \mathbf{e}_f + n_l \mathbf{E}_f^0), \tag{35}$$

where the first term takes care of the gradient of hydrostatic pressure and shear stress:

$$\tau_f = K_f \nabla \cdot \mathbf{u}_f \mathbf{I} - i\omega\eta(\nabla \mathbf{u}_f + \nabla \mathbf{u}_f^T - \tfrac{2}{3}\nabla \cdot \mathbf{u}_f \mathbf{I}),$$

where η is viscosity, while the second term is the force from ions driven by the electric field in the fluid phase. For the solid phase, we have only the stress term,

$$-i\omega\rho_s \dot{\mathbf{u}}_s = \nabla . \tau_s, \tag{36}$$

where

* The last boundary condition should be consistently given by $\mathbf{n} \cdot \mathbf{j}_f = q$ since $\mathbf{j}_f$ is the linearly varying current density carrying $-i\omega t$ time dependence and $Q = Q^0 + q(\omega)e^{-\omega t}$.

$$\tau_s = K_f \nabla . \mathbf{u}_f \mathbf{I} + G(\nabla \mathbf{u}_s + \nabla \mathbf{u}_s^T - \tfrac{2}{3} \nabla \cdot \mathbf{u}_s \mathbf{I}),$$

where G is shear modulus. The boundary conditions are

$$\mathbf{n} \cdot (\tau_s - \tau_f) = -Q^0 \mathbf{e}_s, \tag{37}$$

which states that the stress discontinuity at the interface is due to the stress from the electrostatic force, and the continuity of elastic deformations at the coherent interface:

$$\mathbf{u}_s = \mathbf{u}_f. \tag{38}$$

The macroscopic equations are obtained by coarse-graining the microscopic equations by defining the average of any property $\mathbf{a}_\xi$ of the ξth phase:

$$\langle \mathbf{a}_\xi \rangle = \frac{1}{V_A} \int_{V_\xi} \mathbf{a}_\xi dV, \tag{39}$$

where $\mathbf{V}_A$ is the averaging volume assumed larger than the solid grains but smaller than the acoustic wavelengths, encompassing both solid and fluid phases. For the gradient field we have

$$\langle \nabla \mathbf{a}_\xi \rangle = \nabla \langle \mathbf{a}_\xi \rangle + \frac{1}{V_A} \int_S \mathbf{n}_\xi \mathbf{a}_\xi dA, \tag{40}$$

where $\mathbf{n}_f = \mathbf{n}$ and $\mathbf{n}_s = -\mathbf{n}$. Since we have fluid and solid phases, porosity is defined as

$$\phi = \frac{V_f}{V_A}. \tag{41}$$

We further define an intensive phase average:

$$\bar{\mathbf{a}}_\xi = \langle \mathbf{a}_\xi \rangle / \varphi_\xi, \tag{42}$$

where φ_ξ is the volume fraction of the ξth phase:

$$\varphi_\xi = V_\xi / V_A,$$

and total average:

$$\bar{\mathbf{A}} = \sum_\xi \langle \mathbf{a}_\xi \rangle = \sum_\xi \varphi_\xi \bar{\mathbf{a}}_\xi. \tag{43}$$

Clearly, the porosity is given by $\phi = \varphi_f$, so that $\varphi_s = 1 - \phi$.

The averaging process will produce the following results for the solid phase

$$\nabla \cdot \langle \mathbf{e}_s \rangle = 0, \tag{44}$$

$$\nabla \cdot \langle \mathbf{b}_s \rangle = 0, \tag{45}$$

$$\nabla \times \langle \mathbf{e}_s \rangle = i\omega\mu_0 \langle \mathbf{h}_s \rangle, \tag{46}$$

$$\nabla \times \langle \mathbf{h}_s \rangle = -i\omega\varepsilon_0\kappa_s \langle \mathbf{e}_s \rangle, \tag{47}$$

while for the fluid phase,

$$\varepsilon_0\kappa_0 \nabla \cdot \langle \mathbf{e}_f \rangle = \sum_l ez_l \langle n_l \rangle, \tag{48}$$

$$\nabla \cdot \langle \mathbf{b}_f \rangle = 0, \tag{49}$$

$$\nabla \times \langle \mathbf{e}_f \rangle = i\omega\mu_0 \langle \mathbf{h}_f \rangle, \tag{50}$$

$$\nabla \times \langle \mathbf{h}_f \rangle = -i\omega\varepsilon_0\kappa_f \langle \mathbf{e}_f \rangle + \langle \mathbf{j}_f \rangle, \tag{51}$$

where

$$\langle \mathbf{j}_f \rangle = \sum_l ez_l [-D_l \langle \nabla n_l \rangle + ez_l b_l N_l^0 \langle \mathbf{e}_f \rangle + ez_l b_l \mathbf{E}_f^0 \langle n_l \rangle + N_l \langle \dot{\mathbf{u}}_f \rangle].$$

Hence, our macroscopic Maxwell's equations are rewritten here:

$$\nabla \cdot \overline{\mathbf{D}} = \phi \sum_l ez_l \overline{n}_l, \tag{52}$$

$$\nabla \cdot \overline{\mathbf{B}} = 0, \tag{53}$$

$$\nabla \times \overline{\mathbf{E}} = i\omega \overline{\mathbf{B}}, \tag{54}$$

$$\nabla \times \overline{\mathbf{H}} = -i\omega \overline{\mathbf{D}} + \phi(\overline{\mathbf{J}}_d + \overline{\mathbf{J}}_s + \overline{\mathbf{J}}_n + \overline{\mathbf{J}}_c). \tag{55}$$

Since the interface is assumed to be in a chemical equilibrium, the interface diffusion current, $\mathbf{J}_n$, is assumed to be negligible. This situation is expected to change if there are chemical reactions at the interface. If we start from the conservation of charges of ions:

$$\sum_l ez_l N_l = \text{constant},$$

then we have

$$\sum_l ez_l (i\omega \overline{n}_l + D_l \nabla^2 \overline{n}_l) = \nabla \cdot (\mathbf{J}_c + \mathbf{J}_s + \mathbf{J}_n),$$

where the right hand side simply accounts for the transport mechanisms other than the diffusion in order to preserve the total number of charges. We want to show that the left hand side is negligible by forming a dimensionless number:

$$\frac{\left|D_l \nabla^2 \overline{n}_l\right|}{i\omega \overline{n}_l} \approx \frac{D_l \lambda^{-2}}{\omega} = \frac{D_l f}{2\pi c^2} \tag{56}$$

since the wavelength λ is related to the frequency $\omega = 2\pi f$ through $c = f\lambda$. Typical values are $D_l = 10^{-5}$ cm^2/s at room temperature, c = 10^5 cm/s, and $f = 10 - 10^6$ Hz, making the diffusion current negligible. Hence, we are left with the conduction current $\mathbf{J}_c$ and the streaming current $\mathbf{J}_s$ as the two dominant charge transport mechanisms.

SUMMARY

The macroscopic Maxwell's equations show a linear dependence on porosity ϕ. The dominant charge transport mechanisms are conduction current and streaming current. Both transport mechanisms can be induced by acoustic wave perturbation. Simultaneous measurement of the coupled electromagnetic and seismic wave allows calculation of the transfer functions between seismic and electric and magnetic fields. These transfer functions are a function of electrical and mechanical properties of the pore-fluid and solid matrix.

In homogeneous multi-layer media, two types of seismoelectric signals are generated. In homogeneous porous medium, propagation of seismic wave generates a stationary charge separation. This charge separation produces an internal constant electric field confined within and traveling with the seismic wave. A second type seismoelectric response is generated when the seismic wave crosses an interface between two homogeneous porous media having contrast in mechanical or electrical properties. It gives rise to an electromagnetic emission at the layer interface, which would be detected almost simultaneously across the surface receivers.

Processing of the seismoelectric data is required to enhance small amplitude of the seismoelectric responses. Processing procedure includes removal of the powerline harmonic interference as well as the separation of two different seismoelectric response types. Block or sinusoid subtraction technique can be used to suppress the powerline harmonics. The F-K filtering or self-deconvolved prediction error filter could be used to discriminate between two seismoelectric responses. In practice, the later technique should have better performance compared to the F-K transformation because the small amplitude of the interface EM response at large offsets could restrict efficiency of the F-K filtering.

REFERENCES

Beamish, D., and Peart, R.J., 1998, Electrokinetic geophysics – a review: Terra Nova, **10**, 48-55.

Biot, M.A., 1956, Theory of propagation of elastic waves in a fluid saturated porous solid: I. Low frequency range. J. Acoust. Soc. Am., **28**, 168-178.

Biot, M.A., 1962, Mechanics of deformation and acoustic propagation in porous media: J. Appl. Phys., **33**, 1482-1498.

Butler, K.E., and Russell, R.D., 1993, Subtraction of powerline noise from geophysical records: Geophysics, **58**, 898-903.

Garambois, S. and Dietrichz, M., 2001, Seismoelectric wave conversions in porous media: Field measurements and transfer function analysis: Geophysics, **66**, 1417-1430.

Haartsen, M.W., and Pride, S.R., 1997, Electroseismic waves from point sources in layered media: J. Geophys. Res., **102**, 24745–24769.

Mikhailov, O.V., Queen J., and Toksoz M.N., 2000, Using borehole electroseismic measurements to detect and characterize fractured (permeable) zones: Geophysics, **65**, 1098-1112.

Pride S.R., 1994, Governing equations for the coupled electromagnetics and acoustics of porous media: Phys. Rev. B., **50**, 15678-15696.

Pride S.R., and Haartsen M.W., 1996, Electroseismic wave properties: J. Acoust. Soc. Am., **100**, 1301-1315.

Soubaras, R., 1994, Signal-preserving random noise attenuation by the F-X projection: 64th Ann. Internat. Mtg, Soc. Expl. Geophys., Expanded Abstracts, 1576–1579.

Thompson, A.H., and Gist, G.A., 1993, Geophysical applications of electrokinetic conversion: The Leading Edge, **12**, 1169-1173.

Yoshida, S., Uyeshima, M., and Nakatani, M., 1997: Electric potential charges associated with slip failure of granite: preseismic and coseismic signals: J. Geophys. Res., **102**, 14883–14897.

van Dedem, E., and Verschuur, D., 2001, 3-D surface multiple prediction using sparse inversion: 71st Ann. Internat. Mtg, Soc. Expl. Geophys., Expanded Abstracts, 1285–1288.